Block Precoding for MUI/ISI-Resilient Generalized Multicarrier CDMA With Multirate Capabilities

Zhengdao Wang, *Student Member, IEEE,* and Georgios B. Giannakis, *Fellow, IEEE*

***Abstract*—Potential increase in capacity along with the need to provide multimedia services and cope with multiuser interference (MUI) and intersymbol interference (ISI) arising due to wireless multipath propagation, motivate well multirate wideband code-division multiple-access (CDMA) systems. Unlike most existing continuous-time symbol-periodic and multipath-free studies, the present paper develops an all-digital block-precoded filterbank framework capable of encompassing single- or multirate transceivers for asynchronous or quasi-synchronous CDMA transmissions through multipath channels. Thanks to symbol blocking and through appropriate design of user codes, the resulting generalized multicarrier (GMC) CDMA system not only subsumes known multicarrier CDMA variants, but also equips them with flexible multirate capabilities. It is computationally simple, and guarantees symbol recovery regardless of the (possibly unknown) FIR multipath channels in both downlink and uplink setups. Simulations corroborate that the novel GMC-CDMA system outperforms existing multirate alternatives in the presence of asynchronism and multipath, and illustrate the feasibility of recovering blindly multirate transmissions received through unknown frequency-selective channels in the uplink. Performance of GMC-CDMA system in UMTS channels is also simulated and compared with existing multirate schemes.**

***Index Terms*—Blind equalization, multicarrier transmission, multicode, multipath fading channels, multirate CDMA, variable spreading length.**

I. Introduction

RECENTLY there has been an increasing interest in providing multirate services to wireless communicators. Examples of such services include text, images, data, and low rate video. These services entail variable rates and may have different Quality of Service (QoS) requirements. Future wireless communication systems should thus support flexible QoS and rate-scalability. In addition, third generation multirate systems should have low complexity and exhibit resilience to MUI and ISI caused by multipath propagation.

Multirate services can be provided in many ways. Among them code-division multiple-access (CDMA) systems have attracted much attention thanks to their design flexibility and potential for improved capacity. Using direct-sequence (DS) CDMA, multirate services may be offered by choosing appropriately: chip rate, variable spreading length (vsl), number of multiple codes (mc), and/or modulation format [19]. As a special case of vsl-CDMA, the so called Orthogonal Variable Spreading Factor (OVSF) codes were favored in the third-generation (3G) standard, despite their sensitivity to multipath that causes nonnegligible cross-correlations among the received coded sequences.[1] Adopting OVSF codes in orthogonal frequency division multiple access (OFDMA) enables MUI-free multirate transmissions regardless of multipath channels [24]. However, user symbol recovery is not guaranteed and the system in [24] requires tight quasi-synchronism to offer high bandwidth efficiency. In addition, similar to vsl-CDMA schemes, the users' rates in OVSF-OFDMA can only be some special integer divisors (e.g., 1/2, 1/4, ...) of the highest rate present in the system.

At the receiver end, multirate DS-CDMA systems may include: maximum-likelihood (ML) decoders [18], conventional matched filters (MF), decorrelating or zero-forcing (ZF) multichannel equalizers [15], [22], minimum mean-square error (MMSE) receivers [2], successive interference cancellers (SIC), and decision feedback (DF) receivers [1]. In the absence of multipath, performance of multirate DS-CDMA has been studied for both synchronous and asynchronous systems [3], [15]. Much of the existing multipath-free analysis focuses on asymptotic performance measures such as asymptotic multiuser efficiency [2], [3]. Other works on multirate CDMA systems include rate-compatible error control (channel) coding [7], network layer protocols [20], and QoS issues [13].

MUI and ISI affect critically the capacity and performance of a CDMA system. MUI gives rise to near–far problems and although receiver designs (ZF, MMSE, or ML) can alleviate MUI, they often come at the price of noise enhancement and/or high complexity. Even worse, there may be cases where multiuser symbols are not even recoverable from the received signal when users experience asynchronous and/or (perhaps unknown) multipath channels that cause ISI [30, p. 37]. The recently proposed generalized multicarrier[2] (GMC) CDMA scheme [10], [30] is a mutually orthogonal usercode-receiver (AMOUR) system that addresses such problems for a *single-rate* system, where MUI/ISI-free transmissions are achieved in a quasi-synchronous multipath environment, while at the same time blind symbol recovery is guaranteed with a linear receiver regardless of frequency-selective multipath. In

Paper approved by G. E. Corazza, the Editor for Spread Specturm of the IEEE Communications Society. Manuscript received October 30, 1999; revised August 21, 2000 and February 25, 2001. This work was supported by NSF CCR Grant 98-05350 and NSF Wireless Initiative Grant 99-79443. This paper was presented in part at the International Conference on Communications, New Orleans, LA, June 18–22, 2000.

The authors are with the Department of Electrical and Computer Engineering, University of Minnesota, Minneapolis, MN 55455 USA (e-mail: zhengdao@ece.umn.edu; georgios@ece.umn.edu).

Publisher Item Identifier S 0090-6778(01)10172-8.

[1]Cell-specific scrambling codes are overlaid on the transmitted signal, but the system still relies on the orthogonality among OVSF codes to demodulate.

[2]We abbreviate multicarrier as MC and multicode as mc to avoid confusion.

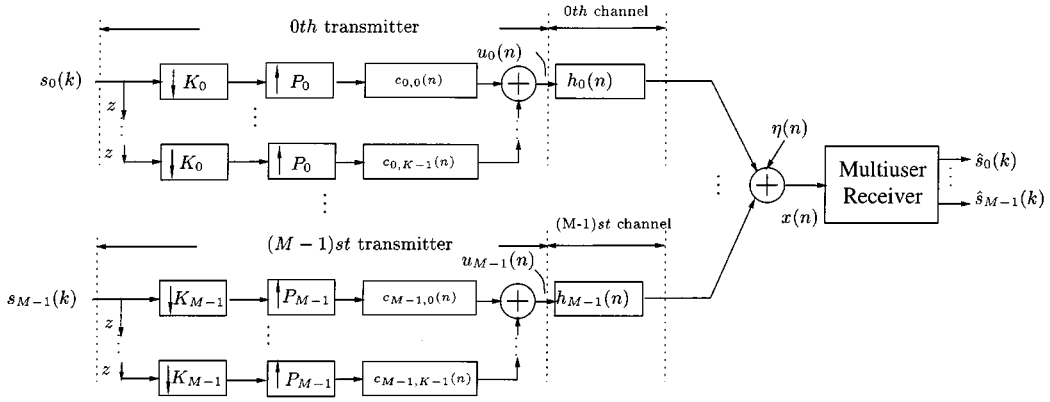

Fig. 1. Multirate block-precoded CDMA system.

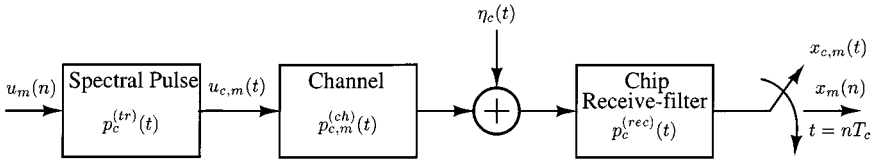

Fig. 2. Baseband continuous-time model for user m, sampled at the chip rate; $p_c^{(tr)}(t)$, $p_{c,m}^{(ch)}(t)$, $p_c^{(rec)}(t)$ denote, respectively, the transmit-chip waveform, the mth user's channel, and the receive-chip waveform.

this paper, we develop an important *multirate* generalization to the AMOUR system, which preserves all its properties while being able to accommodate users of different rates. As we will demonstrate throught simulations, GMC-CDMA outperforms existing mc and vsl in both time-invariant and time-varying (as those specified by the UMTS standard) multipath channels.

The novelties and contents of this paper are organized in three stages. First, we develop an all-digital filterbank-based multirate GMC-CDMA model which can describe both mc and vsl schemes in the general asynchronous multipath scenario (Section II). Next, we focus on quasi-synchronous GMC-CDMA transmissions in multipath. Based on the quasi-synchronous multirate model, we derive and evaluate a novel MUI/ISI-resilient multirate GMC-CDMA system, which has low complexity, fine rate resolution, and easy rate switching capabilities (Section III). Third, we evaluate performance of various linear receivers (MF, ZF, or MMSE) for two multirate CDMA schemes, namely mc and vsl, in the presence of multipath and compare them with that of our proposed system as well (Section IV).

II. The GMC-CDMA Multirate Model

Wideband multicarrier transmissions have received considerable attention recently, particularly for high data rate applications, thanks to their robustness in the presence of frequency-selective fading channels [4], [6], [11]. Although many existing works adopt continuous-time models to describe multicarrier transmissions in multipath, generalizing [26] and [6, pp. 3–12] (which considered single-rate symbol-level spreading only), we will develop an all-digital baseband equivalent *block-spreading* model and illustrate its unifying merits and practical implications. Specifically, we shall generalize here the symbol-periodic, single-rate, single-carrier (SC) CDMA filterbank of [6], [26], to a block-precoded multirate GMC-CDMA system model. It will turn out that our GMC-CDMA model encompasses mc/vsl-CDMA, and a host of existing CDMA schemes (see also [8], [29]). The model will also suggest the multirate AMOUR system of Section III.

We assume that: **as1)** There are *maximum* M users in the system. The chip interval is common to all users; i.e., $T_{c,\mu} = T_c,\ \forall \mu \in [0, M-1]$, where μ is the generic user index; i.e., all users spread their information symbols over the same bandwidth. We will also focus on a single-cell setup, absorbing inter-cell interference in the additive background noise.

A. Multirate Transmitter Filterbank Design

Under as1), the composite received signal from all users can be filtered and sampled at the same rate, usually at the common chip rate. If the radio frequency (RF) signal bandwidth is less than or equal to $1/T_c$ (due to filtering, like in IS-95), then the Nyquist rate of the received complex signal envelope will be $\leq 1/T_c$, and chip-rate sampling will entail no loss of information; otherwise, oversampling can be used. Our subsequent developments will rely upon the discrete-time baseband equivalent chip rate model of Fig. 1 which is reached after baseband filtering and chip rate sampling (see also Fig. 2). Generalization to oversampling receivers is possible but will not be pursued due to lack of space.

Fig. 1 is a discrete-time filterbank multiple access block-transmission model, which generalizes the single rate filterbank model proposed in [10]. Note that as in [10] and [26] the FIR channels include both multipath and asynchronism among users. Each user μ groups the information symbols $s_\mu(k)$ in blocks of length K_μ, and then spreads each of the K_μ symbols using a distinct code of length P_μ implemented in Fig. 1 by

the FIR filters $c_{\mu,k}(n)$, $k = 0, 1, \ldots, K_\mu - 1$, to produce the transmitted signal (chip rate)[3]:

$$u_\mu(n) = \sum_{i=-\infty}^{\infty} \sum_{k=0}^{K_\mu - 1} s_\mu(iK_\mu + k) c_{\mu,k}(n - iP_\mu). \quad (1)$$

Note that K_μ in (1) determines not only the number of symbols per information block, but also the number of codes utilized by user μ. Hence, the spreading factor for user μ is P_μ/K_μ chips per symbol. The sequence $u_\mu(n)$ goes through the Linear Time Invariant (LTI) channel represented in Fig. 1 by its impulse response $h_\mu(n)$, assumed to be FIR of order L_μ. Channels $\{h_\mu(n)\}_{\mu=0}^{M-1}$ are assumed to vary slow enough so that during one observation interval they remain essentially unchanged and therefore they can be modeled as time-invariant. Allowing for user-dependent channels covers the general uplink setup and subsumes the downlink scenario where each user receives the superimposed transmissions through its own (but yet a single) channel $h_\mu(n) = h(n), \forall \mu \in [0, M-1]$. With $\eta(n)$ denoting the filtered/sampled noise, the composite received signal from all M users is

$$\begin{aligned} x(n) &= \sum_{\mu=0}^{M-1} x_\mu(n) + \eta(n) \\ &= \sum_{\mu=0}^{M-1} u_\mu(n) * h_\mu(n) + \eta(n) \\ &= \sum_{\mu=0}^{M-1} \sum_{i=-\infty}^{\infty} \sum_{k=0}^{K_\mu - 1} s_\mu(iK_\mu + k) \tilde{c}_{\mu,k}(n - iP_\mu) + \eta(n) \end{aligned} \quad (2)$$

where $\tilde{c}_{\mu,k}(n) := (c_{\mu,k} * h_\mu)(n)$, and "$*$" stands for convolution. The symbol-spread, single-rate filterbank model of [26] follows as a special case of (2) with $K_\mu = 1$ and $P_\mu = P$, $\forall \mu \in [0, M-1]$. Model (2) also encompasses the block-spread single-rate filterbank transmitter of [10] which corresponds to choosing $K_\mu = K > 1$ and $P_\mu = P, \forall \mu \in [0, M-1]$.

For user μ, a block of K_μ symbols is transmitted using P_μ chips. We thus define the information rate of user μ to be

$$R_\mu = \frac{K_\mu}{P_\mu T_c} \quad (3)$$

which has units of symbols/second. In order to incorporate variable rate services, we have three options: i) fix $P_\mu = P, \forall \mu$, and vary K_μ; ii) fix $K_\mu = K, \forall \mu$, and vary P_μ; iii) vary both K_μ and P_μ. In an mc-CDMA system (see, e.g., [18]), high rate users are allocated a large number of codes (large K_μ) and each high rate symbol is spread by a different code but of the same code length P. This follows as a special case of our model corresponding to option i).

In a vsl-CDMA system, the spreading code lengths P_μ for different rate users are different, but K_μ is kept the same ($K_\mu = 1, \ \forall \mu$), which corresponds to option ii). We will show that with lcm denoting least common multiple and $P = lcm(P_0, \ldots, P_{M-1})$, one can view the vsl-CDMA (option ii) and the multirate option iii) as special cases of the mc-CDMA scheme, where each user spreads information symbols using multiple codes, which are time-shifted versions of a common shorter code. Letting $i = qQ_\mu + r$ with $Q_\mu := P/P_\mu$ and $r \in [0, Q_\mu - 1]$, we can re-write (1) as

$$u_\mu(n) = \sum_{q=-\infty}^{\infty} \sum_{r=0}^{Q_\mu - 1} \sum_{k=0}^{K_\mu - 1} s_\mu(qQ_\mu K_\mu + rK_\mu + k) \, c_{\mu,k}(n - qQ_\mu P_\mu - rP_\mu). \quad (4)$$

If we change variables to $\tilde{k} = rK_\mu + k$, $\tilde{K}_\mu = Q_\mu K_\mu$, and select the mc codes: $c_{\mu,\tilde{k}}^{(mc)}(n) \equiv c_{\mu,k}(n - rP_\mu)$ for $\tilde{k} \in [0, \tilde{K}_\mu - 1]$, we can write $u_\mu(n)$ in (4) as $\sum_{q=-\infty}^{\infty} \sum_{\tilde{k}=0}^{\tilde{K}_\mu - 1} s_\mu(i\tilde{K}_\mu + \tilde{k}) c_{\mu,\tilde{k}}^{(mc)}(n - qP)$, which establishes that vsl-CDMA (option ii) and the general multirate (option iii) are special cases of mc-CDMA (option i). Bearing in mind the practical differences between options i–iii in terms of demodulation delay and implementation complexity, which have been treated in e.g., [19], [22], the unifying viewpoint offers us important mathematical and conceptual conveniences and a general framework for studying and comparing the different multirate schemes. To illustrate this viewpoint, we depict in Fig. 3(b) a vsl user with $K_\mu = 1$ possessing spreading codes $c_{\mu,0}(n)$ of length $P_\mu = 4$, viewed as an equivalent mc user possessing $\tilde{K}_\mu = 4$ codes each of length $P = 16$, with the 4 codes being $c_{\mu,0}(n)$, $c_{\mu,1}(n) = c_{\mu,0}(n-4)$, $c_{\mu,2}(n) = c_{\mu,0}(n-8)$, $c_{\mu,3}(n) = c_{\mu,0}(n-12)$, each of which is zero-padded to have length $P = 16$ [cf. Fig. 3(a)].

We can now summarize our first result as follows.

Result 1: The all-digital, block-precoded, multirate CDMA transmission model of (1) includes as special cases: 1) the conventional symbol-periodic, single-rate filterbank CDMA model of [26]; 2) the existing symbol-periodic mc and vsl multirate CDMA models of [7], [15], [18], [22], [28]; and 3) the recent block-precoded single-rate AMOUR system of [10].

Notice that in contrast to the general model in Fig. 1, multirate models in e.g., [22] restrict the code length in the mc system to be an integer multiple of the vsl system; hence, users are only allowed to have rates that are integer divisors of the highest rate present. Furthermore, [22] deals with *synchronous multipath-free* CDMA only.

Although the scalar model is already complete in describing our multirate transmission system, we introduce the vector counterpart of (2) to facilitate the receiver design. We group the input sequences $s_\mu(n)$ into blocks of length K_μ (^{T} stands for transpose) $\boldsymbol{s}_\mu(i) := [s_\mu(iK_\mu), \ldots, s_\mu(iK_\mu + K_\mu - 1)]^T$, and the transmitted sequences $u_\mu(n)$ into blocks of length P_μ: $\boldsymbol{u}_\mu(i) := [u_\mu(iP_\mu), \ldots, u_\mu(iP_\mu + P_\mu - 1)]^T$. By setting $n = iP_\mu + p$, $0 \le p \le P_\mu - 1$ in (1) and taking into account the fact that $c_{\mu,k}(n) = 0$ for $n \notin [0, P_\mu - 1]$, we obtain $u_\mu(iP_\mu + p) = \sum_{k=0}^{K_\mu - 1} s_\mu(iK_\mu + k) c_{\mu,k}(p)$. Therefore, the block-spreading operation of user μ can be described by the linear mapping

$$\boldsymbol{u}_\mu(i) = \boldsymbol{C}_\mu \boldsymbol{s}_\mu(i), \quad (5)$$

[3]Throughout this paper, arguments n, k, i will denote, respectively, chip, symbol, block-of-symbols indexes.

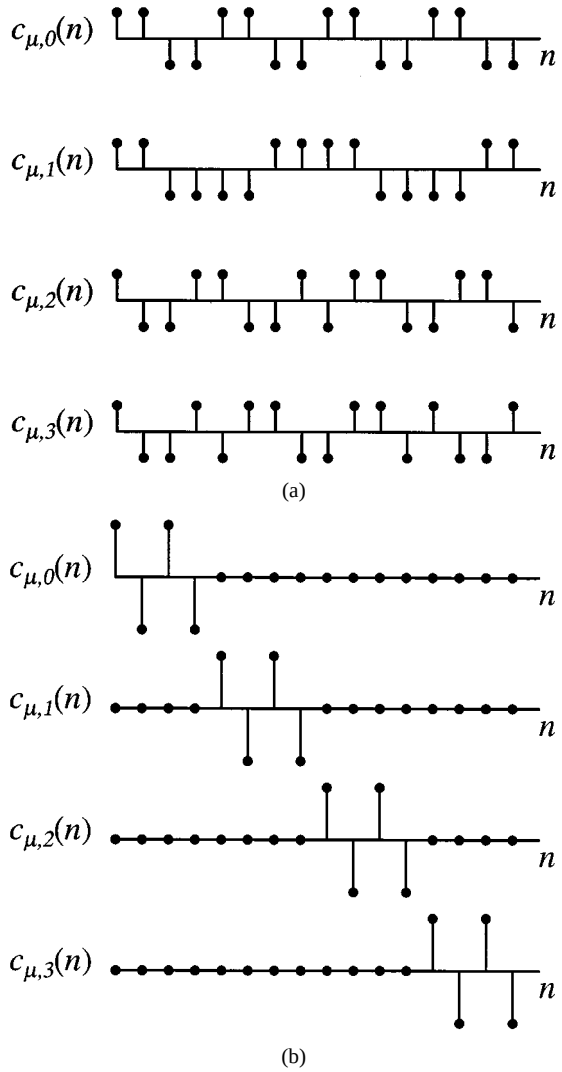

Fig. 3. Multirate schemes. (a) mc and (b) vsl.

where $\boldsymbol{C}_\mu := [\boldsymbol{c}_{\mu,0} \cdots \boldsymbol{c}_{\mu,K_\mu-1}]$ and $\boldsymbol{c}_{\mu,k} := [c_{\mu,k}(0) \cdots c_{\mu,k}(P_\mu-1)]^T$.

Having established our block-precoded multirate transmitter vector model and its relationships with existing single- and multirate CDMA transmissions, we now move on to the design of our multirate receiver.

B. Asynchronous Multirate Receiver Design

With $x(n)$ of (2) as their input, several receiver options are possible (see e.g., [28]): i) ML; ii) MF; iii) ZF; iv) MMSE ; v) variations of the above (e.g., adaptive and DF receivers). In this paper, we will focus on the low-complexity linear receivers ii)–iv) only.

To allow for asynchronous multirate transmissions through multipath channels, we will consider N consecutive blocks of P received chips, where N corresponds to the receiver memory expressed in P-long blocks. Over NP chips, the μth user sends $NP/P_\mu = Q_\mu N$ blocks of K_μ symbols: $\overline{\boldsymbol{s}}_{\mu,N} := [\boldsymbol{s}_\mu^T(0) \cdots \boldsymbol{s}_\mu^T(Q_\mu N-1)]^T$, which are spread first to produce

$$\begin{aligned}\overline{\boldsymbol{u}}_{\mu,N} &:= [\boldsymbol{u}_\mu^T(0) \cdots \boldsymbol{u}_\mu^T(Q_\mu N-1)]^T \\ &= (\boldsymbol{I}_{Q_\mu N} \otimes \boldsymbol{C}_\mu)\overline{\boldsymbol{s}}_{\mu,N} \end{aligned} \tag{6}$$

where $\boldsymbol{I}_{Q_\mu N}$ denotes an identity matrix of dimension $Q_\mu N \times Q_\mu N$, and in deriving (6) we used (5) and the definition of the Kronecker product "$\otimes$." The received block $\tilde{\boldsymbol{x}}_N := [x(0) \cdots x(NP-1)]^T$ consists of NP chips and can be written as [cf. (5)]

$$\tilde{\boldsymbol{x}}_N = \sum_{\mu=0}^{M-1} \mathbf{H}_{\mu,N}(\boldsymbol{I}_{Q_\mu N} \otimes \boldsymbol{C}_\mu)\overline{\boldsymbol{s}}_{\mu,N} + \tilde{\boldsymbol{\eta}}_N \tag{7}$$

where $\mathbf{H}_{\mu,N}$ is an $NP \times NP$ channel-induced lower triangular Toeplitz convolution matrix with first column $[h_\mu(0), \ldots, h_\mu(L_\mu), 0, \ldots, 0]$, and $\tilde{\boldsymbol{\eta}}_N$ is an $NP \times 1$ vector denoting additive Gaussian noise. To avoid Inter-Block Interference (IBI), we discard chips after NP, because their impact is negligible if one collects sufficient blocks to assure that $NP \gg L_\mu, \forall \mu$. Notice that the multipath model (7) does not bound asynchronism among the users. If user (quasi--) synchronism [17] can be assumed, IBI can be removed either by appending trailing zeros at end of the codes $c_{\mu,k}(n)$, or, by employing receivers with leading zeros (as in OFDM) to discard the cyclic prefix appended per transmitted block (see also [10], [23], [24], [30] for detailed derivations).

Letting $\overline{\boldsymbol{C}}_{\mu,N} := \mathbf{H}_{\mu,N}(\boldsymbol{I}_{Q_\mu N} \otimes \boldsymbol{C}_\mu)$ and $\tilde{\boldsymbol{s}}_N := [\overline{\boldsymbol{s}}_{0,N}^T, \ldots, \overline{\boldsymbol{s}}_{M-1,N}^T]^T$, we can also write (7) as

$$\tilde{\boldsymbol{x}}_N = \left[\overline{\boldsymbol{C}}_{0,N} \cdots \overline{\boldsymbol{C}}_{M-1,N}\right] \tilde{\boldsymbol{s}}_N + \tilde{\boldsymbol{\eta}}_N := \tilde{\boldsymbol{C}}_N \tilde{\boldsymbol{s}}_N + \tilde{\boldsymbol{\eta}}_N. \tag{8}$$

Based on the vector model (8), a general linear FIR receiver can be described by the matrix $\boldsymbol{G}_N$ of dimension $(N \cdot \sum_{\mu=0}^{M-1} Q_\mu K_\mu) \times NP$ as follows:

$$\hat{\tilde{\boldsymbol{s}}}_N := \boldsymbol{G}_N \tilde{\boldsymbol{x}}_N = \boldsymbol{G}_N \tilde{\boldsymbol{C}}_N \tilde{\boldsymbol{s}}_N + \boldsymbol{G}_N \boldsymbol{\eta}_N \tag{9}$$

where $\hat{\tilde{\boldsymbol{s}}}_N$ is the estimated symbol vector defined similar to $\tilde{\boldsymbol{s}}_N$. Note that all elements of $\hat{\tilde{\boldsymbol{s}}}_N$ are not equally reliable; those on either end of $\tilde{\boldsymbol{s}}_N$ may not be as accurately estimated as those in the middle, because the symbols in the middle part are more correlated with the remaining symbols in the $\tilde{\boldsymbol{s}}_N$ block due to the channel memory. In practice, we may use a sliding window of length $N\sum_{\mu=0}^{M-1} Q_\mu K_\mu$ to process $\tilde{\boldsymbol{x}}_N$. But instead of estimating all N blocks of symbols jointly, we can only estimate the middle block, which amounts to choosing the middle $\sum_{\mu=0}^{M-1} Q_\mu K_\mu$ rows of $\boldsymbol{G}_N$. After sliding the window by $\sum_{\mu=0}^{M-1} Q_\mu K_\mu$, we estimate the next block of length $\sum_{\mu=0}^{M-1} Q_\mu K_\mu$, and so on.

Depending on how we select $\boldsymbol{G}_N$ in (9), we obtain different linear receivers. Possible choices are the MF and ZF receivers given by [$^{\mathcal{H}}$ stands for Hermitian transpose and $(\cdot)^\dagger$ denotes pseudoinverse]: $\boldsymbol{G}_N^{mf} = \tilde{\boldsymbol{C}}_N^{\mathcal{H}}$, $\boldsymbol{G}_N^{zf} = \tilde{\boldsymbol{C}}_N^\dagger$; and with $\boldsymbol{R}_s := E[\tilde{\boldsymbol{s}}_N(i)\tilde{\boldsymbol{s}}_N^{\mathcal{H}}(i)]$ and $\boldsymbol{R}_\eta := E[\tilde{\boldsymbol{\eta}}_N(i)\tilde{\boldsymbol{\eta}}_N^{\mathcal{H}}(i)]$, the MMSE receiver $\boldsymbol{G}_N^{mmse} = \boldsymbol{R}_s \tilde{\boldsymbol{C}}_N^{\mathcal{H}}(\boldsymbol{R}_\eta + \tilde{\boldsymbol{C}}_N \boldsymbol{R}_s \tilde{\boldsymbol{C}}_N^{\mathcal{H}})^{-1}$.

We have seen in (5) that our filterbank transmitter performs a linear mapping from the $K_\mu \times 1$ block of information symbols $\boldsymbol{s}_\mu(i)$ to the $P_\mu \times 1$ transmitted sequence $\boldsymbol{u}_\mu(i)$. Such a linear mapping model is quite general and encompasses many existing CDMA schemes by specializing $\boldsymbol{C}_\mu$. Those include single-carrier (SC) DS-CDMA [28], multicarrier (MC) CDMA [11], MC-DS-CDMA [16], and MT-CDMA [27] (see [8] and references therein).

III. MUI/ISI-Free Multirate Transmissions

Our derivation of the ZF (a.k.a decorrelating) receivers in the previous section assumed that the matrix inverse $\tilde{\boldsymbol{C}}_N^{\dagger}$ exists. Unlike CDMA systems that rely on symbol-spread codes, the AMOUR system proposed in [10] guarantees (even blind) recovery of the user symbols regardless of the (possibly unknown) Lth-order multipath channels, by specially designing long spreading sequences $c_{\mu,k}(n)$. Unlike long random codes that rely on power control to suppress MUI statistically, MUI in block-spread CDMA (like AMOUR) is eliminated deterministically by applying a simple linear transformation on the received sequence.

It is practically important to carry these desirable MUI/ISI-elimination features over to our multirate GMC-CDMA system described in Section II-A. In view of Result 1 and the unifying merits of our model [8], [29], [30], derivation of a rate-scalable GMC-CDMA system equips all-digital multicarrier CDMA transceivers with multirate capabilities.

A. Quasi-Synchronous Multirate Transceiver Design

The basic idea behind GMC-CDMA is to build user code polynomials specified by distinct sets of what we term *signature points* on the complex plane. Users' codes are constructed such that their $\mathcal{Z}$-transforms are zero at other users' signature points and nonzero at each user's own signature points. Specifically, define the code polynomial $C_{\mu,k}(z) := \sum_{n=0}^{P_\mu} c_{\mu,k}(n)z^{-n}$ and let each user be given distinct signature points $\{\rho_{\mu,j}\}_{j=0}^{J-1}$, where J is a design parameter. It is then possible to construct codes such that $\forall\, k, \forall\, j$, [10]

$$C_{\mu,k}(\rho_{m,j}) = \begin{cases} 0, & \text{if } \mu \neq m \\ A_\mu f_{\mu,k,j}, & \text{if } \mu = m \end{cases} \tag{10}$$

where $f_{m,k,j}$ are nonzero constants up to the designer's choice and A_μ controls the μth user's transmitted power. The minimum-length codes $c_{\mu,k}(n)$ come from polynomials $C_{\mu,k}(z)$ that have degree $MJ-1$ [10]. With L denoting an upper bound on all channel orders ($L \geq L_\mu, \forall\, \mu$), we append L trailing zeros (guard chips) at the end of those codes $c_{\mu,k}(n)$ thereby augmenting their length to $P = MJ + L$. Because each of the M users in the single-rate system of [10] transmits K information symbols with codes of length P, the system's bandwidth efficiency is $\mathcal{E} := MK/P$ and approaches 1, provided that one selects $J = K + L$ and block lengths $K \gg L$. In addition to as1), we now also assume the following.

as2) The system is quasi-synchronous, and the underlying FIR channels have maximum order $L = \tilde{L} + D$ which incorporates the maximum order $\tilde{L}$ of the chip-sampled multipath channels and the maximum delay $D \ll P = MJ+L$ that arises due to relative asynchronism among users. Our user codes $c_{\mu,k}(n)$ have length P and include L trailing zeros; i.e., $c_{\mu,k}(n) = 0$ for $n \notin [0,\, MJ-1]$.

With T_c denoting the chip/sampling-period, $\tau_{\max,s}$ denoting the maximum delay spread and $\tau_{\max,d}$ denoting the maximum relative delay among the users, L in **as2)** is found as $L = \lceil(\tau_{\max,s} + \tau_{\max,d})/T_c\rceil$, where $\lceil\cdot\rceil$ stands for integer-ceiling; $\tau_{\max,d}$ can be computed from the cell-size while $\tau_{\max,s}$ can be obtained from field measurements of the operational environment. Typical delay spread values for various environments are also well documented (see e.g., [21]). With these notional prerequisites, we summarize the basic result from [10] in the following.

Theorem 1 (`single-rate AMOUR [10]`)*:* Under as1), **as2)** and for a given L, choose user codes $c_{\mu,k}(n)$ with length $P = MJ + L$, where $J = K + L$. For a prescribed bandwidth efficiency $\mathcal{E} \in (0, 1)$, select symbol blocking of size $K = L(1 + 1/M)\mathcal{E}/(1 - \mathcal{E})$. Mutually orthogonal code matrices $\boldsymbol{C}_\mu$ [cf. (5)] having corresponding polynomials $C_{\mu,k}(z)$ obeying (10) with appropriately chosen $f_{\mu,k,j}$, and zero-forcing receivers $\boldsymbol{G}_\mu^{zf}$ [cf. (9)] then exist that eliminate MUI and ISI deterministically by design and regardless of the (possibly unknown) multipath channels $h_\mu(n)$. Transmit redundancy enables (even blind) channel estimation independent of the symbol constellation used and the location of channel zeros.

Actually, due to **as2)** the channels are of the form

$$H_\mu(z) := \sum_{l=0}^{L} h_\mu(l)z^{-l} = z^{-d}\sum_{l=0}^{\tilde{L}} h(l+d)z^{-l} \tag{11}$$

where $0 \leq d \leq D$. Therefore, they can have at most $\tilde{L}$ finite roots per channel. As a result, the condition $J = K+L > L$ in [10] for guaranteeing blind channel identifiability and symbol recovery can be relaxed to $J = K + \tilde{L} > \tilde{L}$. Note that in this latter case, each user can transmit $K_\mu = K = J - \tilde{L}$ symbols per $P_\mu = P$ chips; therefore, the μth user has rate $R_\mu = R = K/(PT_c), \forall\, \mu$. The total rate R_T is thus

$$R_T := \sum_{\mu=0}^{M-1} R_\mu = \frac{MK}{T_cP} = \frac{M(J-\tilde{L})}{T_c(MJ+L)} \tag{12}$$

which can be made as close to $1/T_c$ as one chooses by sufficiently increasing J.

In the derivation of the single-rate AMOUR system, the quasi-synchronous assumption **as2)** has been adopted. Although more restrictive than full asynchronism, quasi-synchronism (or bounded asynchronism) is more relaxed than the synchronous case and can indeed be satisfied easily in practice. Furthermore, thanks to block-spreading, the amount of asynchronism that can be tolerated can be as much as a few symbols. This is quite feasible even with existing systems such as IS-95. For example, consider a cell of radius 5 km and chip rate 1.2288 mega chips per second with spreading gain 64. The maximum relative delay between the base station and the mobiles is about 33 μs or 40 chips. Considering multipath delay spread of 20 μs (worst channel in a UMTS vehicular environment [5, p. 43]), amounts to about 25 chips. Thus, the total amount of asynchronism (relative delay plus multipath) can be 65 chips or about one symbol. Among users, the asynchronism can be at most twice as much, i.e., 2 symbols. Besides, if the system can afford a little extra bandwidth, or, if the system is not fully loaded as in a number of applications, the subcarriers in GMC-CDMA can be sufficiently separated so that they remain (even approximately) orthogonal in an FDMA-like sense, and then additional (or even full) asynchronism is allowed.

Having clarified the practical merits of quasi-synchronous GMC-CDMA for single-rate users, we now return to the multirate scenario. To accommodate different rates, a multicode (mc) approach is possible. Specifically, one can split each high rate user's symbol stream into several low rate substreams, so that each spread substream is treated as if it corresponded to a virtual user. But in this way, the available rates can take only multiple values of a minimum rate $R = K/(PT_c)$, i.e., one of $\{R, 2R, \ldots, MR\}$. We say that the rate resolution in this case is R.

To achieve finer resolution, we can allocate different numbers J_μ of signature points to different users instead of the same number J used in [10]. Suppose there are a *total number* of J_T signature points, where J_T is a design parameter. We can allocate J_μ signature points to user μ, subject to the constraints: i) $J_\mu > \tilde{L}$; ii) $\sum_{\mu=0}^{M-1} J_\mu = J_T$. From Theorem 1 and the discussion following it, we know that constraint i) guarantees symbol recovery even in the presence of frequency-selective multipath channels.

With J_μ signature points, the μth user can transmit $K_\mu = J_\mu - \tilde{L}$ symbols with $P = J_T + L$ chips; therefore, the rate of user μ now becomes $R_\mu = (J_\mu - \tilde{L})/(PT_c)$, and as before, the total rate

$$R_T = \frac{J_T - M\tilde{L}}{PT_c} = \frac{J_T - M\tilde{L}}{(J_T + L)T_c} \tag{13}$$

can be made as close to $1/T_c$ as one wishes by simply increasing J_T. There are tradeoffs in selecting J_T though: larger J_T implies higher total rate but also longer decoding delay and increased susceptibility to Doppler effects and/or carrier offsets, as there will be more (J_T) subcarriers within a fixed bandwidth ($\approx 1/T_c$). Other tradeoffs such as peak-to-average power ratio and system loading that were discussed in [10] and [9] for the single-rate ($J_\mu = J$) AMOUR system apply here as well.

In summary, to equip our GMC-CDMA system with multirate capabilities, we follow these design steps:

S1) Choose $J_T \gg L$ so that $\sum_{\mu=0}^{M-1} R_\mu$ comes close to the available bandwidth $1/T_c$, while respecting a prescribed decoding delay.

S2) For each user μ, allocate J_μ of the J_T signature points so that R_μ is close to the μth user's desired rate.

S3) Design user codes $c_{\mu,k}(n)$ so that their polynomials $C_{\mu,k}(z)$ satisfy [cf. (10)]

$$C_{\mu,k}(\rho_{m,j}) = A_\mu \rho_{\mu,j}^{-k} \delta(\mu - m) \tag{14}$$

where the choice $f_{m,j,k} = \rho_{m,j}^{-k}$ in (10) will be appreciated in the next subsection and is further motivated in [10], [30]. Specifically, we start with points $\rho_{m,j}$ on the complex plane, and using Lagrange interpolation [25, pp. 329–332], we obtain the user code polynomials that satisfy (14) as

$$C_{\mu,k}(z) = A_\mu \sum_{\lambda=0}^{J_\mu - 1} \rho_{\mu,\lambda}^{-k} \prod_{\substack{m=0 \\ (m,j)\neq(\mu,\lambda)}}^{M-1} \prod_{j=0}^{J_m - 1} \frac{1 - \rho_{m,j} z^{-1}}{1 - \rho_{m,j}\rho_{\mu,\lambda}^{-1}}. \tag{15}$$

S4) Design the receiver using any of the structures in Section II-B with $N = 1$. □

Thanks to the L guard chips that we appended in our user codes [as per **as2)**], there is no IBI between successively received P-long blocks. With white AGN and independent transmitted blocks, the received blocks are independent, which explains why designing a receiver with memory $N = 1$ incurs no loss of optimality in S4).

We now proceed to show that the so designed multirate system inherits the MUI/ISI-free properties of [10], [30] and guarantees multipath-irrespective recovery of the user symbols. Since $P_\mu = P, \forall\, \mu$, (8) simplifies to

$$\tilde{\boldsymbol{x}} = [\mathbf{H}_0 \boldsymbol{C}_0 \cdots \mathbf{H}_{M-1} \boldsymbol{C}_{M-1}]\, \tilde{\boldsymbol{s}} + \tilde{\boldsymbol{\eta}} \tag{16}$$

where we have omitted the subscript N for simplicity. Note that only the symbols in the first ($i = 0$) block are involved in $\tilde{\boldsymbol{s}}$.

Let $\mathbf{G}_{vd}$ denote the $J_T \times P$ Vandermonde matrix constructed from all signature points

$$\mathbf{G}_{vd} := [\boldsymbol{v}_P(\rho_{0,0}) \cdots \boldsymbol{v}_P(\rho_{0,J_0}) \cdots \boldsymbol{v}_P(\rho_{M-1,0}) \cdots \boldsymbol{v}_P(\rho_{M-1,J_{M-1}})]^T \tag{17}$$

where $\boldsymbol{v}_P(\rho_{\mu,k}) := [1\, \rho_{\mu,k}^{-1} \cdots \rho_{\mu,k}^{1-P}]^T$. It can be readily verified that multiplying $\mathbf{G}_{vd}$ with a vector is equivalent to evaluating the vector's $\mathcal{Z}$-transform at the users' signature points. In particular, because $\boldsymbol{v}_P^T(\rho_{\mu,k})\mathbf{H}_m = H_m(\rho_{\mu,k})\boldsymbol{v}_P^T(\rho_{\mu,k})$, it follows from (16) and (17) that

$$\begin{aligned} \tilde{\boldsymbol{y}} &:= \mathbf{G}_{vd}\tilde{\boldsymbol{x}} = \mathbf{G}_{vd}\,[\mathbf{H}_0 \boldsymbol{C}_0 \cdots \mathbf{H}_{M-1}\boldsymbol{C}_{M-1}]\, \tilde{\boldsymbol{s}} + \mathbf{G}_{vd}\tilde{\boldsymbol{\eta}} \\ &= \left[\, \overline{\mathbf{H}}_0 \mathbf{G}_{vd}\boldsymbol{C}_0 \cdots \overline{\mathbf{H}}_{M-1}\mathbf{G}_{vd}\boldsymbol{C}_{M-1} \right] \tilde{\boldsymbol{s}} + \mathbf{G}_{vd}\tilde{\boldsymbol{\eta}} \end{aligned} \tag{18}$$

where we used that $\mathbf{G}_{vd}\mathbf{H}_\mu = \overline{\mathbf{H}}_\mu \mathbf{G}_{vd}$ with $\mathbf{H}_\mu$ as in (7), and

$$\overline{\mathbf{H}}_\mu := \mathrm{diag}[H_\mu(\rho_{0,0}), \ldots, H_\mu(\rho_{0,J_0-1}), \ldots, H_\mu(\rho_{M-1,0}), \ldots, H_\mu(\rho_{M-1,J_{M-1}-1})].$$

Taking into account the code design step S3), we further obtain

$$\begin{aligned} \mathbf{G}_{vd}\boldsymbol{C}_\mu &= \begin{bmatrix} C_{\mu,0}(\rho_{0,0}) & \cdots & C_{\mu,K_\mu-1}(\rho_{0,0}) \\ \vdots & \vdots & \vdots \\ C_{\mu,0}(\rho_{0,J_0-1}) & \cdots & C_{\mu,K_\mu-1}(\rho_{0,J_0-1}) \\ \vdots & \vdots & \vdots \\ C_{\mu,0}(\rho_{M-1,0}), & \cdots, & C_{\mu,K_\mu-1}(\rho_{M-1,0}) \\ \vdots & \vdots & \vdots \\ C_{\mu,0}(\rho_{M-1,J_{M-1}-1}) & \cdots & C_{\mu,K_\mu-1}(\rho_{M-1,J_{M-1}-1}) \end{bmatrix} \\ &= A_\mu \begin{bmatrix} \mathbf{0}_{\mu 1} & \boldsymbol{F}_\mu^T & \mathbf{0}_{\mu 2} \end{bmatrix}^T \end{aligned} \tag{19}$$

where

$\mathbf{0}_{\mu 1}$ all zero matrix of size $(\sum_{m=1}^{\mu-1} J_m) \times K_\mu$;

$\mathbf{0}_{\mu 2}$ all zero matrix of size $(\sum_{m=\mu+1}^{M-1} J_m) \times K_\mu$;

$\boldsymbol{F}_\mu$ $J_\mu \times K_\mu$ Vandermonde matrix with (j, k)th entry $\rho_{\mu,j}^{-k}$.

Equation (19) confirms that the transmit- and receive-filters $\boldsymbol{C}_\mu$ and $\boldsymbol{G}_\mu$ are designed *mutually orthogonal* for channel-transparent MUI elimination and explains the name AMOUR of our system.

Defining $S_\mu(z) := \sum_{n=0}^{K_\mu-1} s_\mu(n) z^{-n}$, the matrix equation (18) is simplified to [cf. (19)]

$$\tilde{\boldsymbol{y}} = A_\mu \begin{bmatrix} H_0(\rho_{0,0}) S_0(\rho_{0,0}) \\ \vdots \\ H_0(\rho_{0,J_0-1}) S_0(\rho_{0,J_0-1}) \\ \vdots \\ H_{M-1}(\rho_{M-1,0}) S_{M-1}(\rho_{M-1,0}) \\ \vdots \\ H_{M-1}(\rho_{M-1,J_{M-1}-1}) S_{M-1}(\rho_{M-1,J_{M-1}-1}) \end{bmatrix} + \mathbf{G}_{vd}\tilde{\boldsymbol{\eta}} \quad (20)$$

which proves that our multirate GMC-CDMA code design has achieved user separation at the signature points. For the μth user, $S_\mu(z)$ is of degree $K_\mu - 1$ unless $S_\mu(z) \equiv 0$; therefore, $S_\mu(z)$ has at most $K_\mu - 1$ finite roots. We know from (11) that $H_\mu(z)$ can have at most $\tilde{L}$ finite roots. Therefore, $H_\mu(z)S_\mu(z)$ can have at most $K_\mu - 1 + \tilde{L} := J_\mu - 1$ roots. It follows that if $S_\mu(z) \not\equiv 0$, at least one of $H_\mu(\rho_{\mu,j})S_\mu(\rho_{\mu,j})$ must be nonzero for $j = 0, 1, \ldots, J_\mu - 1$. To establish identifiability of users' symbols from $\tilde{\boldsymbol{y}}$ (and hence from $\tilde{\boldsymbol{x}}$) in the absence of noise, we argue by contradiction supposing that there exist two distinct symbol sets $\tilde{\boldsymbol{s}}^{(1)} \not\equiv \tilde{\boldsymbol{s}}^{(2)}$ that yield $\tilde{\boldsymbol{y}}^{(1)} \equiv \tilde{\boldsymbol{y}}^{(2)}$. But (20) implies that $H_\mu(\rho_{\mu,j})[S_\mu^{(1)}(\rho_{\mu,j}) - S_\mu^{(2)}(\rho_{\mu,j})] \equiv 0, \forall \mu \in [0, M-1]$ and $j \in [0, J_\mu - 1]$, which is impossible because the $S_\mu(z) := S_\mu^{(1)}(z) - S_\mu^{(2)}(z) \not\equiv 0$.

As with single user OFDM, (20) shows that GMC-CDMA converts a frequency selective channel to a set of flat-fading subchannels. But unlike OFDM, where the user's symbols are directly put on different subcarriers, we place linearly precoded (combined) symbols $S_\mu(\rho_{m,j})$ on the subcarriers. That way, each symbol is spread on multiple subcarriers and frequency diversity is therefore accomplished (see also [31]). The distinct advantage of our system compared to mc/vsl systems that exploit multipath diversity (the time-domain counterpart of frequency diversity), comes from the block-spreading used in GMC-CDMA to enable MUI and ISI elimination by design (recall that MUI and ISI are two major performance-limiting factors of mc/vsl systems). The performance edge of GMC-CDMA over mc and vsl systems will be further verified by the simulations of Section IV. In addition to the linear precoding (over the complex field) that is offered by block-spreading, finite-field channel coding can also be used to improve performance with the corresponding increase in bandwidth and/or complexity. Preliminary comparisons of block coding for error control with GMC-CDMA's block-precoding/spreading approach were carried in [9]. Thorough analysis and optimum combination of block spreading with error-control coding is a deep subject and goes beyond the scope of this paper (see [31] for preliminary results).

Going back to (20) and using the same technique as in [10] one can apply further linear transformations on $\tilde{\boldsymbol{y}}$ to establish that the multirate users can be isolated not only at their signature points but also on the entire $\mathcal{Z}$-plane, implying that our code design in (15) allows multiple users to transmit through their own single user equivalent channels. Specifically, by applying the inverse of the $J_\mu \times J_\mu$ Vandermonde matrix $\mathbf{V}_\mu$, whose (i, j)th entry is $\rho_{\mu,i}^{-j}$, on the MUI-free vector $\tilde{\boldsymbol{y}}_\mu := [H_\mu(\rho_{\mu,0})S_\mu(\rho_{\mu,0}) \cdots H_\mu(\rho_{\mu,J_\mu-1})S_\mu(\rho_{\mu,J_\mu-1})]^T$, one obtains from (20) the $J_\mu \times 1$ time-domain block

$$\boldsymbol{y}_\mu := \mathbf{V}_\mu^{-1}\tilde{\boldsymbol{y}}_\mu = A_\mu \tilde{\mathbf{H}}_\mu \boldsymbol{s}_\mu + \mathbf{V}_\mu^{-1}\mathbf{G}_{vd}\tilde{\boldsymbol{\eta}} \quad (21)$$

where $\tilde{\mathbf{H}}_\mu$ is a $J_\mu \times K_\mu$ Toeplitz convolution matrix with first row $[h_\mu(0)\, 0 \cdots 0]$ and first column $[h_\mu(0) \cdots h_\mu(L_\mu - 1)\, 0 \cdots 0]^T$. Based on $\boldsymbol{y}_\mu$, the channel taps $h_\mu(n)$ can be estimated even blindly (up to a scalar) by applying signal/noise subspace decomposition techniques on the autocorrelation matrix of $\boldsymbol{y}_\mu$ after prewhittening it. Single user equalizers $\boldsymbol{\Gamma}_\mu$ of size $K_\mu \times J_\mu$ can then be applied once the channel has been estimated (see [10] for details).

Notice that the Toeplitz matrix $\tilde{\mathbf{H}}_\mu$ is always full rank (unless the channel taps are all zero, which is impossible). That means a ZF equalizer ($\boldsymbol{\Gamma}_\mu = A_\mu^{-1}\tilde{\mathbf{H}}_\mu^\dagger$) based on $\boldsymbol{y}_\mu$ always exists and symbol recovery can therefore be guaranteed. Equation (21) also establishes that after MUI elimination, the multiple access channel has been converted to parallel single user channels. Since matrix $\mathbf{V}^{-1}$ is always nonsingular, applying it as in (21) does not entail any loss of information. Because $\mathbf{V}^{-1}$ is generally nonunitary, noise enhancement will result. However, it can be alleviated if one employs a single user (such as MMSE) equalizer to account for the noise color. It is also possible to apply the matrix equalizer directly on the received vector $\tilde{\boldsymbol{x}}$ as we mentioned in S4).

After applying the single user equalizer (e.g., MMSE) $\boldsymbol{\Gamma}_\mu$ to the MUI-free vector $\boldsymbol{y}_\mu$ in (21), we can write the symbol estimates as

$$\hat{\boldsymbol{s}}_\mu = A_\mu \boldsymbol{\Gamma}_\mu \tilde{\mathbf{H}}_\mu \boldsymbol{s}_\mu + \boldsymbol{\Gamma}_\mu \mathbf{V}_\mu^{-1}\boldsymbol{G}_{vd}\tilde{\boldsymbol{\eta}} := \boldsymbol{G}_{\mu,1}\boldsymbol{s}_\mu + \boldsymbol{G}_{\mu,2}\tilde{\boldsymbol{\eta}}. \quad (22)$$

If the entries of $\boldsymbol{s}_\mu$ are binary (± 1) i.i.d., the average bit error rate (BER) after hard decision on $\hat{\boldsymbol{s}}_\mu$ can be found to be (see the Appendix):

$$P_{e,\mu} = \frac{1}{K_\mu} \sum_{k=0}^{K_\mu-1} \frac{1}{2\pi j} \int_{c-j\infty}^{c+j\infty} \nu^{-1} \Upsilon_{\mu,k}^{\mathrm{sym}}(\nu) \cdot \Upsilon_{\mu,k}^{\mathrm{isi}}(\nu) \Upsilon_{\mu,k}^{\mathrm{noise}}(\nu)\, d\nu \quad (23)$$

where $c > 0$, $\Upsilon_{\mu,k}^{\mathrm{sym}}(\nu) := \exp(-[\boldsymbol{G}_{\mu,1}]_{k,k} \cdot \nu)$, $\Upsilon_{\mu,k}^{\mathrm{isi}}(\nu) := \prod_{i=0, i\neq k}^{K_\mu-1} \cosh([\boldsymbol{G}_{\mu,1}]_{k,i} \cdot \nu)$ and $\Upsilon_{\mu,k}^{\mathrm{noise}}(\nu) := \exp((\sigma^2\nu^2/2)\sum_{p=0}^{P-1} |[\boldsymbol{G}_{\mu,2}]_{k,p}|^2)$; $[\cdot]_{a,b}$ stands for the

(a, b)th entry of a matrix. The integrals in (23) can be evaluated efficiently using numerical methods along a path of steepest descent (by choosing c) in the integrand (see [12] for detailed derivations). A closed-form BER expression is possible and has been derived in [10] when the ZF equalizer is adopted instead of the MMSE.

We summarize our results on multirate MUI/ISI-resilient GMC-CDMA transceiver design in the following theorem.

Theorem 2 (multirate GMC-CDMA): Given channel parameters $\tilde{L}$, D, and users of prescribed rates $R_0, \ldots, R_{M-1}$ that satisfy $R_T = \sum_{\mu=0}^{M-1} R_\mu < 1/T_c$, choose $J_T > (LT_cR_T + M\tilde{L})/(1 - T_cR_T)$ such that: $J_T = \sum_{\mu=0}^{M-1} J_\mu$, $(J_\mu - \tilde{L})/PT_c > R_\mu$, and select $P = J_T + L$. Under as1) and **as2)**, MUI/ISI-resilient transmissions at or above the specified rates are then possible regardless of FIR multipath channels up to order $L = \tilde{L} + D$ with guaranteed (even blind) channel identifiability and symbol recovery.

Because $P_\mu = P, \ \forall \mu$, we note that $R_\mu = K/(PT_c)$ in (3), and from Theorem 1 we infer that in order to guarantee MUI/ISI-resilient symbol recovery, we must have $J_\mu \in [K_\mu + \tilde{L}, \ J_T]$; i.e., since $K_\mu \geq 1$, a specific user can be allocated from $1 + \tilde{L}$ to J_T signature points. Therefore, each user's rate can be any one of

$$\left\{ \frac{1}{PT_c}, \frac{2}{PT_c}, \ldots, \frac{J_T - \tilde{L}}{PT_c} \right\}.$$

The rate resolution in this case is $1/(PT_c)$, which is K times finer than the virtual user approach discussed after Theorem 1 and can be made small if we choose P large, or equivalently J_T large.

As far as complexity is concerned, GMC-CDMA in its full generality requires multiplication by the MUI-eliminating $J_T \times P$ matrix $\boldsymbol{G}_{vd}$, followed by M single-user equalizers $\boldsymbol{\Gamma}_\mu$ (of size $K_\mu \times J_\mu$ for the μth user) applied, respectively, on $\boldsymbol{y}_\mu$, $\mu = 0, \ldots, M-1$. Compared to an mc- or a vsl-CDMA system of spreading gain P, which in the presence of multipath would require the inversion of a $P \times P$ matrix, our system has less complexity.

Having presented our general rate-scalable MUI/ISI-resilient GMC-CDMA system design along with its fine rate resolution capabilities, we now consider a low-complexity special case of it.

B. Multirate AMOUR—A Special Case

We consider here a special case of the proposed system, where the users' signature points are chosen equispaced on the unit circle. Let us define the set of FFT frequencies

$$\mathcal{F} = \{ c^{j(2\pi/J_T)l}, \ l = 0, 1, \ldots, J_T - 1 \} \tag{24}$$

and let $\{\mathcal{F}_\mu\}_{\mu=0}^{M-1}$ be a partitioning of $\mathcal{F}$ into nonintersecting subsets, with each subset $\mathcal{F}_\mu$ containing J_μ distinct complex exponentials; i.e., $\bigcup_{\mu=0}^{M-1} \mathcal{F}_\mu = \mathcal{F}$, $\mathcal{F}_\mu \cap \mathcal{F}_m = \emptyset, \forall \mu \neq m$ and $\sum_{\mu=0}^{M-1} J_\mu = J_T$. The subset $\mathcal{F}_\mu$ contains user μ's signature points. Unlike the complex signature points allowed for GMC-CDMA, such unit-modulus signature points not only enable low-complexity FFT-based processing [10], but as we will see next, they bear direct correspondence to physical frequencies.

Taking into account the fact that the last L taps (chips) of $c_{\mu,k}(n)$ are zero as per **as2)**, the right $P \times L$ submatrix of $\mathbf{G}_{vd}$ in (17) is zero, while its left part with the signature points in (24) becomes equivalent to a $P \times P$ FFT matrix. From (19), we see that

$$\mathbf{G}_{vd} \boldsymbol{C}_\mu \boldsymbol{s}_\mu(i) = \begin{bmatrix} \mathbf{0}_{\mu 1} \\ \boldsymbol{F}_\mu \\ \mathbf{0}_{\mu 2} \end{bmatrix} \boldsymbol{s}_\mu(i) \tag{25}$$

where $\boldsymbol{F}_\mu$ performs FFT on the information symbol block and (25) indicates that the Fourier transform of the μth user's transmitted sequence $\boldsymbol{u}_\mu(i) = \boldsymbol{C}_\mu \boldsymbol{s}_\mu$ will be zero at the other users' signature points and $S_\mu(\rho_{\mu,j}) \neq 0$ at its own signature points $\rho_{\mu,j}$, $j = 0, 1, \ldots, J_\mu - 1$. This offers an equivalent implementation of the multirate AMOUR system as shown in Fig. 4, which in the special case of $K_\mu = 1$ reduces to an MC-CDMA system, [4], [6], [11], with the spreading code vector in the frequency domain being $\tilde{\mathbf{c}}_\mu := [\tilde{c}_\mu(0), \ldots, \tilde{c}_\mu(J_T - 1)]^T$. Specifically, if we view the different signature points as sub-carriers, this equivalent implementation shows that our multirate GMC-CDMA system with signature points selected as in (24) reduces to a multirate multicarrier CDMA system, where the μth user's code vector $\tilde{\mathbf{c}}_\mu$ in the frequency domain has entries satisfying

$$\tilde{c}_\mu(l) = \begin{cases} 1, & \text{if } c^{j(2\pi/J_T)l} \in \mathcal{F}_\mu \\ 0, & \text{otherwise} \end{cases}$$
$$\forall \, l = 0, 1, \ldots, J_T - 1. \tag{26}$$

The users' frequency domain signatures in this special form of GMC-CDMA do not overlap, and are orthogonal in a noncontiguous FDMA-like sense. Since the time-domain convolutive multipath channels are multiplicative in the frequency domain, this orthogonality will be preserved at the receiver no matter what the channels' impulse responses are, as long as they are FIR of order $\leq L$. This is precisely what guarantees channel-irrespective MUI elimination in our code design. Moreover, by allocating $\tilde{L}$ additional subcarriers per user, the users' symbols are guaranteed to be recoverable (identifiable), because the channel's transfer function can at most have $\tilde{L}$ finite nulls. As the signature points in our GMC-CDMA system can be any complex number and the users' frequency domain signatures may in general overlap, the low-complexity (FFT-based) AMOUR system of [10] is indeed a special case of our GMC-CDMA system herein.

Notice that once J_T points are selected as in (24), the signatures of the users can be efficiently represented by a J_T-bit frequency domain signature vector $\tilde{\mathbf{c}}_\mu$, with J_μ entries equal to 1 and $J_T - J_\mu$ entries equal to zero. Frequency (or subcarrier) allocation therefore amounts to partitioning the J_T signature points $\mathcal{F}$ and distributing the distinct frequency domain signature vector $\tilde{\mathbf{c}}_\mu$ to different users. The users will then need to

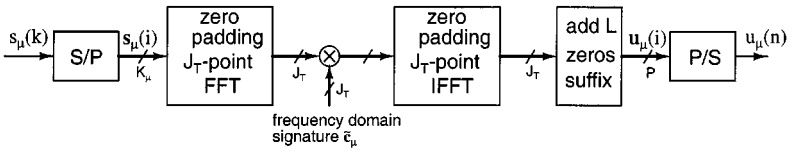

Fig. 4. Equivalent transmitter in the special case of (24).

adjust their signature $\check{\mathbf{c}}_\mu$ accordingly (see Fig. 4). Thanks to the block precoding structure, subcarrier frequencies can be re-allocated even from block to block, which may be particularly attractive for data or video transmission with bursty characteristics. Frequency re-allocation should only affect rate-changing users—the remaining users (majority) can transmit with their already allocated codes. Such dynamic frequency allocation has the potential of maximizing the system throughput and constitutes an interesting future research direction. Also in our future research plans is the resource (code) assignment problem when intra-cell interference is taken into account (instead of being treated as background noise).

IV. Performance Comparisons

In this section, we test mc and vsl schemes for different receivers in the presence of asynchronism and multipath. We also compare their performance with that of the proposed multirate GMC-CDMA system of Section III. Per channel realization, we will calculate BER based on (23), relying on the numerical integration method developed in [12]. Only in the Test Case 5 we will count the number of errors.

Test Case 1 (`mc Versus vsl Comparisons`)*:* We use random spreading codes to remove code-dependent effects. The spreading length P is chosen to be 16, and the simulation includes $M = P/2 = 8$ users, four of which are single rate users with $R_L = 1/(16T_c)$ symbols/second, and the other four users are double rate users with $R_H = 2R_L$. The system is assumed to be asynchronous, and therefore the maximum delay can be as large as $P - 1$. The channels we adopt are of order $\tilde{L} = 5$ with uncorrelated taps of equal variance zero-mean complex Gaussian random variables (Rayleigh fading). BPSK symbol modulation is used, and the performance measure is BER versus E_b/N_0, where E_b denotes energy per bit (assumed to be the same for all users). The BERs are averaged over 500 channel realizations and also across the users of the same rate that results in BER for: mc high rate users, mc low rate users, vsl high rate users, and vsl low rate users. We focus on the multichannel FIR receivers of Section II-B. It is shown in [14] that with moderate memory-length ($N = 11$ here), the FIR decorrelator (ZF) provides the performance of an IIR decorrelator. Since at high SNR, the MMSE equalizer approaches a decorrelating equalizer, the argument holds true for the MMSE at least for high SNR values, and our simulation also suggests that using longer memory does not lead to significant performance improvement even when multipath is present.

From Fig. 5, we can see that mc- and vsl-CDMA perform similarly for all three equalizers. For the MF receivers, there is a near–far problem (BER error floor), which does not appear in the ZF and the MMSE receivers. Interestingly, similar

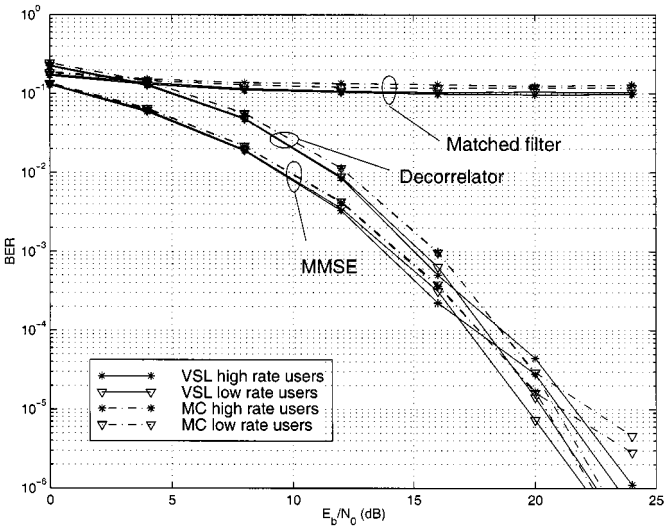

Fig. 5. Performance of mc and vsl.

observations were drawn in [15] in the absence of multipath, and our simulation corroborates [15] even in the presence of asynchronous multipath fading. One can thus conclude that on the average (depending on the code used), mc- and vsl-CDMA do not differ from each other in the presence of multipath fading channels whether or not the transmission is synchronous or asynchronous. We may prefer one over the other considering additional factors such as decoding delay, peak-to-average power ratio, and design flexibility.

Test Case 2 (`Performance of the Multirate AMOUR`)*:* To allow for maximum asynchronism between AMOUR users we choose $D = 15$, and $\tilde{L} = 5$, the same as in the previous simulation. To maintain the same bandwidth occupied by AMOUR and mc/vsl-CDMA, we select $P = 240$ in the AMOUR system, which offers a total of $J_T = P - D - \tilde{L} = 220$ signature points. These signature points are chosen equispaced around the unit circle as in (24). Slow users of rate R_L are allocated $J_L = 20$ signature points each, while fast (high rate) users are given $J_H = 35$ signature points. These choices make the bandwidth efficiency, defined as $\mathcal{E} = R_T T_c$ (the total rate divided by the bandwidth), the same for AMOUR and mc/vsl-CDMA.

Fig. 6 shows the averaged BER for a multirate AMOUR system with $M = 8$ users (4 users with rate R_L and 4 users with double rate $R_H = 2R_L$). We observe that similar to mc/vsl-CDMA, the MMSE equalizers outperform ZF equalizers, while the MF equalizers suffer from the near–far problem as expected. But in the multirate AMOUR, the low rate users exhibit better performance than that of high rate users, because each low rate user is allocated more bandwidth per symbol since $J_L/(J_L - \tilde{L}) > J_H/(J_H - \tilde{L})$. This implies that the

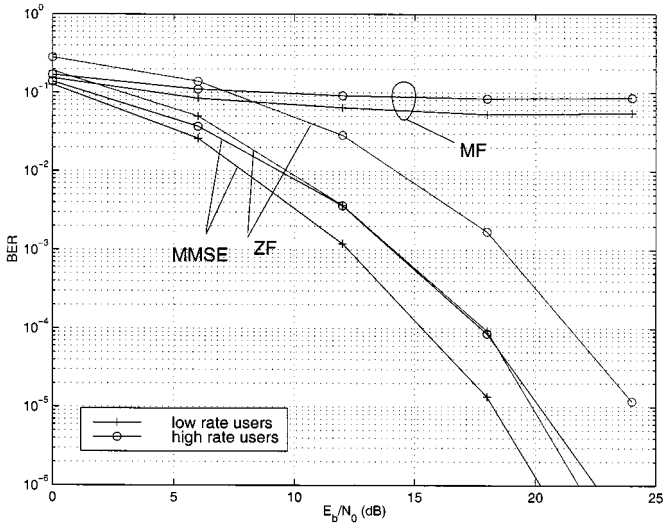

Fig. 6. Performance of multirate AMOUR.

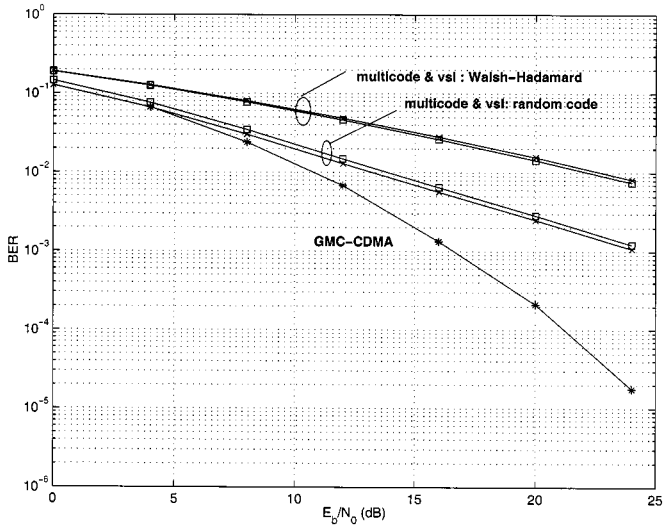

Fig. 7. AMOUR versus mc/vsl-CDMA: $\bar{L} = 1$.

lower rate users can transmit at a lower power level, or alternatively, that the high rate users have to transmit at higher power level to achieve the same performance. As we will illustrate in the next test case, the multirate AMOUR system outperforms mc and vsl CDMA. Therefore, on the average, users in the multirate AMOUR system require less power to achieve the same performance.

Test Case 3 (`Multirate GMC-CDMA Versus mc/vsl-CDMA Comparisons`)*:* In this test, we compare the GMC system of Test Case 2 with *synchronous* mc and vsl systems that have spreading gain 256. Random and Walsh–Hadamard spreading sequences for mc and vsl are simulated and compared with GMC-CDMA codes (we chose spreading $256 > 240 = P$ because W–H sequences of length 256 are easy to generate). Fig. 7 reports MMSE equalization performance for the three systems over 500 random Rayleigh channels of order $\tilde{L} = 1$. The BER for each system is also averaged over high rate users and low rate users. We observe that for all SNR values, the AMOUR system is consistently better than the averaged mc/vsl-CDMA systems, which testifies

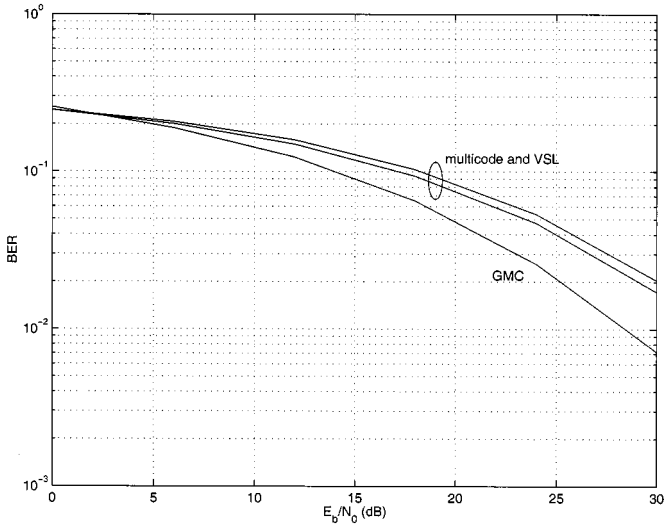

Fig. 8. Performance in UMTS channels.

that multirate AMOUR is more robust to multipath fading than mc/vsl-CDMA (8 dB gain in SNR at $\mathrm{BER} = 10^{-3}$).

Test Case 4 (`Performance in Time-Varying Channels`)*:* Throughout our derivation of GMC-CDMA, we dealt with LTI multipath, which is valid when the channel varies slowly over the duration of one block. To test the robustness of the GMC-CDMA against Doppler effects (or possible carrier offsets), we test its performance using the UMTS channel model specified in [5, sec. B.1.4.2]. The channel has 6 time-varying taps corresponding to paths with relative delays of 0, 300, 8900, 12 900, 17 100, 20 000 nano-seconds, and relative average power -2.5, 0, -12.8, -10.0, -25.2, -16.0 dB, respectively. The Doppler spectrum of each tap is assumed to obey the CLASSIC Clarke–Jakes model [5, sec. B.1.8.2]. Perfect channel information is available to all receivers. Fig. 8 depicts BER curves for the GMC-CDMA and the mc/vsl systems. There are 8 users in the system, 4 high rate users of rate 144 Kbps, and 4 low rate users of rate 72 Kbps. High (low) rate users are allocated 35 (20) subcarriers. Multicode and vsl systems are simulated with random codes of length 240. The carrier frequency is 2 GHz and the speed of the eight users is chosen uniformly distributed between 30 mi/h and 80 mi/h. MMSE receivers are used for all three systems. As we can see, although GMC-CDMA still outperforms the mc/vsl systems, the difference is not as pronounced as in the time-invariant case, which can be explained by the sensitivity to time-selective effects that is common to all multicarrier systems. Detailed study of the performance evaluation of GMC-CDMA through time-varying channels and/or in the presence of carrier offsets deserves further analysis and results will be reported elsewhere.

Test Case 5 (`Multirate AMOUR Performance in Unknown Multipath`)*:* To test the multirate AMOUR performance in unknown multipath, we use the indirect second-order blind equalization method detailed in [10]. The AMOUR system setup is the same as that of Test Case 2. The users are separated first using the $\mathbf{G}_{vd}$ matrix [cf. (17)], and subsequently each user performs blind channel estimation as in [10]. Once individual channels are estimated (up to a scalar ambiguity), a single-user MMSE equalizer is applied. The

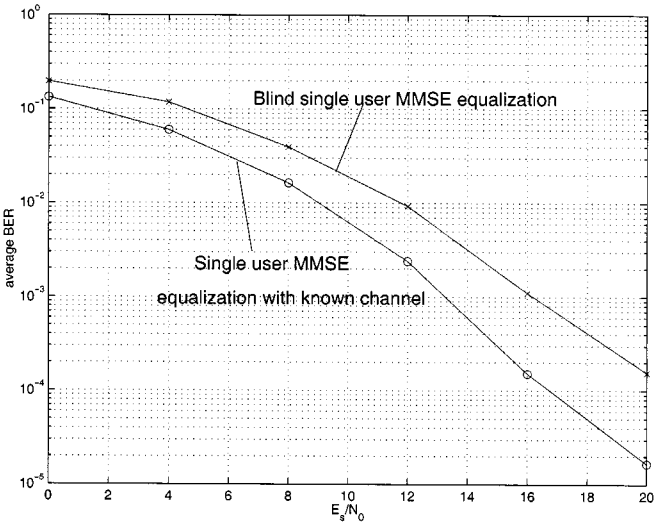

Fig. 9. Blind multirate AMOUR.

single user MMSE equalizer with perfect channel information is used as a reference for comparison. For each user (high or low rate), 100 blocks of symbols are processed by the receiver to estimate the user's channel of order $\tilde{L} = 5$. One hundred Monte Carlo simulations are conducted and their performance is averaged. We observe from Fig. 9 that AMOUR with blind channel estimation performs 2–4 dB below the ideal equalizer. As the number of blocks used for blind channel estimation increases, consistency of the blind channel estimation algorithm guarantees that blind-AMOUR will approach its theoretical performance bound [10].

V. Conclusions and Discussion

In this paper, we introduced a general all-digital multirate generalized multicarrier CDMA model. It relies on symbol blocking and block-precoding, through which a simple form of memory is built to the transmitted sequence that renders decoding computationally simple (only linear operations are needed). We showed that the proposed model unifies the mc/vsl CDMA transmissions in asynchronous multipath settings and encompasses single- and multicarrier CDMA systems including our recent quasi-synchronous AMOUR transceivers in [10]. The model facilitates the multirate receiver design in multipath: matched filters, decorrelating, and minimum mean-square error receivers were designed in matrix forms. More important, our novel framework was also used to derive a multirate GMC-CDMA system, which generalizes our previously designed AMOUR system to incorporate users of different rates. We proved that our multirate GMC-CDMA preserves all the attractive properties of the single-rate AMOUR system, namely deterministic MUI elimination, blind channel estimation and FIR channel-irrespective symbol recovery. It also has fine rate resolution and easy rate switching capability. Through Monte Carlo simulation and by averaging the system performance over frequency-selective Rayleigh fading channels, we have illustrated that the multirate AMOUR system outperforms consistently the best mc/vsl-CDMA systems that use random codes. We have also corroborated through a simple simulation the feasibility of blind equalization with multirate AMOUR transceivers. Surprisingly, although we derived our GMC-CDMA under LTI channel assumptions, the system performs better than existing mc and vsl CDMA systems even in time-varying channels such as those specified by the UMTS standard. For performance comparisons of GMC-CDMA with existing single- and multicarrier CDMA approaches under variable number of active users, the interested reader is referred to [10], [29] and [9], respectively.

Appendix

Supposing that in (22) the symbols of $\boldsymbol{s}_\mu$ are binary (± 1) and iid, we derive here the BER formula (23). Let $[\boldsymbol{v}]_k$ denote the kth entry of a generic vector $\boldsymbol{v}$. The kth entry of $\hat{\boldsymbol{s}}_\mu$ can then be written as [cf. (22)]

$$[\hat{\boldsymbol{s}}_\mu]_k = [\boldsymbol{G}_{\mu,1}]_{k,k}[\boldsymbol{s}_\mu]_k + \sum_{i=0,\, i\neq k}^{K_\mu-1} [\boldsymbol{G}_{\mu,1}]_{k,i}[\boldsymbol{s}_\mu]_i + \sum_{p=0}^{P-1} [\boldsymbol{G}_{\mu,2}]_{k,p}[\tilde{\boldsymbol{\eta}}]_p \quad (27)$$

where $[\boldsymbol{G}]_{k,i}$ denotes the (k, i)th entry of a generic matrix $\boldsymbol{G}$ and the three terms on the right-hand side of (27) correspond, respectively, to the symbol of interest, the ISI and the noise. The BER of the kth symbol $[\boldsymbol{s}_\mu]_k$ can then be expressed as an integral [12]:

$$P_{e,\mu,k} = \frac{1}{2\pi j}\int_{c-j\infty}^{c+j\infty} \nu^{-1}\Upsilon_{\mu,k}^{\mathrm{sym}}(\nu)\Upsilon_{\mu,k}^{\mathrm{isi}}(\nu)\Upsilon_{\mu,k}^{\mathrm{noise}}(\nu)\, d\nu \quad (28)$$

where $c > 0$: $\Upsilon_{\mu,k}^{\mathrm{sym}}(\nu) := \exp(-[\boldsymbol{G}_{\mu,1}]_{k,k}\cdot\nu)$, $\Upsilon_{\mu,k}^{\mathrm{isi}}(\nu) := \prod_{i=0,\, i\neq k}^{K_\mu-1}\cosh([\boldsymbol{G}_{\mu,1}]_{k,i}\cdot\nu)$ and $\Upsilon_{\mu,k}^{\mathrm{noise}}(\nu) := \exp((\sigma^2\nu^2/2)\sum_{p=0}^{P-1}|[\boldsymbol{G}_{\mu,2}]_{k,p}|^2)$. These are the moment-generating functions of the symbol of interest, ISI, and noise terms, respectively. And the integral can be effectively evaluated using the numerical methods detailed in [12]. Equation (23) can be obtained by averaging (28) over the K_μ symbols.

References

[1] S. R. Chaudry and A. U. H. Sheikh, "Performance of a dual-rate DS-CDMA-DFE in an overlaid cellular system," *IEEE Trans. Veh. Technol.*, vol. 48, pp. 683–695, May 1999.

[2] J. Chen and U. Mitra, "MMSE receivers for dual-rate DS/CDMA signals: random signature sequence analysis," in *Proc. IEEE GLOBECOM*, vol. 4, Piscataway, NJ, Nov. 1997, pp. 139–143.

[3] ——, "Analysis of decorrelator-based receivers for multi-rate DS/CDMA communications," *IEEE Trans. Veh. Technol.*, vol. 48, pp. 1966–1983, Nov. 1999.

[4] Q. Chen, E. S. Sousa, and S. Pasupathy, "Multicarrier CDMA with adaptive frequency-hopping for mobile radio systems," *IEEE J. Select. Areas Commun.*, pp. 1852–1857, Dec. 1996.

[5] ETSI. Universal mobile telecommunications system (UMTS); Selection procedures for the choice of radio transmission technologies of the UMTS (UMTS 30.03 version 3.2.0). [Online] TR 101 112 v3.2.0, 04 1998; . Available: http://www.etsi.org/

[6] K. Fazel and G. P. Fettweis, Eds., *Multi-Carrier Spread Spectrum*. Boston, MA: Kluwer Academic, 1997.

[7] P. Frenger, P. Orten, T. Ottosson, and A. Svensson, "Rate-compatible convolutional codes for multirate DS/CDMA systems," *IEEE Trans. Commun.*, vol. 47, pp. 828–836, Aug. 1999.

[8] G. B. Giannakis, P. A. Anghel, and Z. Wang. Wideband generalized multi-carrier CDMA over frequency-selective wireless channels. presented at *Proc. Int. Conf. on ASSP*. [Online]. Available: http://spincom.ece.umn.edu

[9] G. B. Giannakis, A. Stamoulis, Z. Wang, and P. Anghel, "Load-adaptive MUI/ISI-resilient generalized multi-carrier CDMA with linear and decision-feedback equalizers," *Euro. Trans. Telecomm.*, pp. 2501–2504, June 5–9, 2000.

[10] G. B. Giannakis, Z. Wang, A. Scaglione, and S. Barbarossa, "AMOUR—Generalized multicarrier transceivers for blind CDMA regardless of multipath," *IEEE Trans. Commun.*, vol. 48, pp. 2064–2076, Dec. 2000.

[11] S. Hara and R. Prasad, "Overview of multicarrier CDMA," *IEEE Commun. Mag.*, pp. 126–133, Dec. 1997.

[12] C. W. Helstrom, "Calculating error probabilities for intersymbol and cochannel interference," *IEEE Trans. Commun.*, vol. 34, pp. 430–435, May 1986.

[13] M. L. Honig and J. B. Kim, "Allocation of DS-CDMA parameters to achieve multiple rates and qualities of service," in *Proc. IEEE GLOBECOM*, vol. 3, New York, 1996, pp. 1974–1978.

[14] M. J. Juntti and B. Aazhang, "Finite memory-length linear multiuser detection for asynchronous CDMA communications," *IEEE Trans. Commun.*, vol. 45, pp. 611–622, May 1997.

[15] M. J. Juntti and J. O. Lilleberg, "Linear FIR multiuser detection for multiple data rate CDMA systems," in *Proc. Veh. Technol. Conf.*, 1997, pp. 455–459.

[16] S. Kondo and L. B. Milstein, "Performance of multicarrier DS CDMA systems," *IEEE Trans. Commun.*, vol. 44, pp. 238–246, Feb. 1996.

[17] L. Mailaender and R. A. Iltis, "Multiuser detectors with single-user parameter estimation on quasisynchronous CDMA channels," *IEEE Trans. Commun.*, vol. 48, pp. 200–203, Feb. 2000.

[18] U. Mitra, "Comparison of maximum-likelihood-based detection for two multirate access schemes for CDMA signals," *IEEE Trans. Commun.*, vol. 47, pp. 64–77, Jan. 1999.

[19] T. Ottosson and A. Svensson, "On schemes for multirate support in DS/CMDA," *J. Wireless Personal Commun.*, vol. 6, no. 3, pp. 265–287, Mar. 1998.

[20] R. Pichna and Q. Wang, "A medium-access control protocol for a cellular packet CDMA carrying multirate traffic," *IEEE J. Select. Areas Commun.*, vol. 14, pp. 1728–1736, Dec. 1996.

[21] T. S. Rappaport, *Wireless Communications: Principles & Practice*. Englewood Cliffs, NJ: Prentice-Hall, 1996.

[22] M. Saquib and R. Yates, "A two stage decorrelator for a dual rate synchronous DS/CDMA system," in *Proc. Int. Conf. Commun.*, vol. 1, New York, 1997, pp. 334–338.

[23] A. Scaglione, G. B. Giannakis, and S. Barbarossa, "Redundant filterbank precoders and equalizers Part I: Unification and optimal designs," *IEEE Trans. Signal Processing*, vol. 47, pp. 1988–2006, July 1999.

[24] ——, "Lagrange/Vandermonde MUI eliminating user codes for quasisynchronous CDMA in unknown multipath," *IEEE Trans. Signal Processing*, vol. 48, pp. 2057–2073, July 2000.

[25] G. Szego, "Orthogonal polynomials," *Amer. Math. Soc.*, 1975.

[26] M. K. Tsatsanis and G. B. Giannakis, "Optimal decorrelating receivers for DS-CDMA systems: A signal processing framework," *IEEE Trans. Signal Processing*, vol. 44, no. 12, pp. 3044–3055, Dec. 1996.

[27] L. Vandendorpe, "Multitone spread spectrum multiple access communications system in a multipath Rician fading channel," *IEEE Trans. Veh. Technol.*, vol. 44, pp. 327–337, May 1995.

[28] S. Verdú, *Multiuser Detection*. Cambridge, : Cambridge, 1998.

[29] Z. Wang and G. B. Giannakis, "Block spreading for multipath-resilient generalized multi-carrier CDMA," in *Signal Processing Advances in Wireless and Mobile Communications*, G. B. Giannakis, Y. Hua, P. Stoica, and L. Tong, Eds. Englewood Cliffs, NJ: Prentice-Hall, Oct. 2000, vol. II, ch. ch. 6.

[30] ——, "Wireless multicarrier communications: Where Fourier meets Shannon," *IEEE Signal Processing Mag.*, vol. 47, no. 3, pp. 29–48, May 2000.

[31] ——, "Linearly precoded or coded OFDM against wireless channel fades?," in *Proc. IEEE Workshop Signal Processing Adv. Wireless Comm.*, Taoyuan, Taiwan, R.O.C., Mar. 20–23, 2001, pp. 267–270.

Zhengdao Wang (S'00) was born in Dalian, China, in 1973. He received the B.S. degree in electrical engineering and information science from the University of Science and Technology of China (USTC), Hefei, China, in 1996, and the M.Sc. degree in electrical engineering from the University of Virginia, Charlottesville, in 1998.

He is currently working toward the Ph.D. degree with the Department of Electrical and Computer Engineering, University of Minnesota, Minneapolis. His broad interests lie in the areas of signal processing, communications, and computer networks, including cyclostationary signal processing, blind equalization algorithms, transceiver optimization, multicarrier, wideband multiple rate systems, space-time high-rate transmissions, and channel coding. His current interests focus on design and optimization of wireless communication systems.

Georgios B. Giannakis (F'97) received the Diploma in electrical engineering from the National Technical University of Athens, Greece, in 1981. He received the M.Sc. degree in 1983, the M.Sc. degree in mathematics in 1986, and the Ph.D. degree in electrical engineering in 1986, all from the University of Southern California (USC), Los Angeles.

After lecturing for one year at USC, he joined the University of Virginia in 1987, where he became aProfessor of Electrical Engineering in 1997. Since 1999, he has been a Professor with the Department of Electrical and Computer Engineering at the University of Minnesota, where he now olds an ADC Chair in Wireless Telecommunications. His general interests span the areas of communications and signal processing, estimation and detection theory, time-series analysis, and system identification—subjects on which he has published more than 130 journal papers, 270 conference papers, and two edited books. Current research topics focus on transmitter and receiver diversity techniques for single- and multi-user fading communication channels, redundant precoding and space–time coding for block transmissions, multicarrier, and wide-band wireless communication systems.

Dr. Giannakis is a corecipient of three Best Paper Awards from the IEEE Signal Processing (SP) Society (1992, 1998, 2001). He also received the SP Society's Technical Achievement Award in 2001. He coorganized three IEEE-SP Workshops (HOS in 1993, SSAP in 1996 and SPAWC in 1997) and guest coedited four special issues. He has served as an Associate Editor for the IEEE TRANSACTIONS ON SIGNAL PROCESSING, and the IEEE SIGNAL PROCESSING LETTERS, currently serving as Editor-in-Chief, a Secretary of the SP Conference Board, a member of the SP Publications Board, and a member and vice-chair of the Statistical Signal and Array Processing Committee. He is a member of the Editorial Board for the IEEE PROCEEDINGS. He chairs the SP for Communications Technical Committee. He is a member of the IEEE Fellows Election Committee, the IEEE SP Society's Board of Governors, and a frequent consultant for the telecommunications industry.